Relationship between Mesogenic Side Chain Fraction in Liquid Crystalline Copolymer and Bistable Electro-Optical Switching for (Liquid Crystalline Copolymer/Liquid Crystals) Composite Systems

Hirokazu Yamane, Hirotsugu Kikuchi, and Tisato Kajiyama*

Department of Materials Physics and Chemistry, Graduate School of Engineering, Kyushu University, 6-10-1 Hakozaki, Higashi-ku, Fukuoka 812-8581, Japan

Received May 13, 1998; Revised Manuscript Received September 8, 1998

ABSTRACT: The influence of the mesogenic side chain fraction in a side chain liquid crystalline copolymer (LCcoP) on electro-optical effects for (LCcoP/low-molecular-weight nematic liquid crystals (nematic LCs)) composite systems in a smectic state was studied in order to improve reversible and bistable electro-optical switching characteristics driven by ac electric fields with two different frequencies. In the case of the LCcoP fraction lower than 40 wt %, the magnitudes of glass transition temperature (T_g) and the mesophase temperature range for the binary composite systems were independent of the mesogenic side chain fraction in LCcoP, that is, ∼220 K and 220−340 K, respectively. In the case of the LCcoP fraction of 30 wt % and, also, its mesogenic side chain fraction of 52.5 and 32.5 mol %, the binary composite systems showed a homogeneous smectic phase at room temperature. On the other hand, the LCcoP with the mesogenic side chain fraction 16.5 mol % did not exhibit any mesomorphic characteristics at any temperature without any addition of LCs. Then, this LCcoP was named as the pseudo-LCcoP in this study. However, the (pseudo-LCcoP/nematic LCs) composite system showed a novel type of induced smectic phase over a wide range of both mixing concentration (35−85 wt % pseudo-LCcoP) and temperature (220−320 K). This composite system showed a fast switching speed from a transparency state to a light-scattering state. Therefore, it was reasonably concluded that the application of LCcoP with the optimum substituent fraction of mesogenic side chain is useful to realize a high electro-optical switching speed (∼50 ms) as well as a stable memory effect (∼years) at room temperature.

Introduction

Side chain liquid crystalline polymers (LCPs) are interesting and useful materials combining the properties of low-molecular-weight liquid crystals (LCs) such as optical anisotropy, reorientation induced by external stimulations, high mobility, viscous flow, surface-induced orientation, and so forth and also those of polymers such as mechanical toughness, easy fabrication as solid films, and so forth. LCPs are inferior to LCs for the purpose of applications as fast switching electro-optical displays due to their higher viscosity. However, since LCPs have better mechanical stability than LCs due to their higher viscocity, LCPs have been applied as the materials for various types of information storage.[1] Then, erasable information storage can be realized by writing the data at temperatures above T_g and storing the data in a glassy state at temperatures below T_g.[2−4] For this purpose, it is required to synthesize polymers with T_g above room temperature. Also, another technique for storage of optically addressed information has been investigated by using smectic polysiloxanes with T_g below room temperature. In this case, the data were stored in a viscous smectic state, and the integrity of the stable data storage was excellent under ambient conditions.[5−8]

The binary composite systems composed of LCP and LC which has a similar chemical structure to that of the mesogenic side chain in the LCP have been extensively investigated in order to improve the switching speed of LCPs, which exhibit a slower response upon the application of external agencies such as electric or magnetic fields due to their high viscosities.[9−11] The (smectic LCP/nematic LC) composite systems showed faster switching speeds than that for LCP itself because of a remarkable decrease in viscosity. Furthermore, the (smectic LCP/nematic LC) composite system in a compatible smectic state exhibited a reversible and bistable electrooptical switching driven by ac electric fields with two different frequencies,[11−13] as shown in Figure 1. The smectic binary composite system exhibited reversible transparent and light-scattering states upon the application of an ac electric field with a high frequency (∼kHz) and upon the application of one with a low frequency (∼Hz) or dc, respectively. Each transparent and turbid state was stably memorized after the removal of electric fields due to the mechanical strength of smectic layers in the composite systems. It is reasonable to consider that the turbid and transparent states might occur from the balance between the electric current effect based on the electrohydrodynamic motion of the LCP main chains and the electric field effect based on the dielectric anisotropy of the LC molecules and the side chain part of the LCP.

To prepare the smectic binary composite systems with a faster bistable switching speed and a stable memory effect at room temperature, the composite systems composed of smectic liquid crystalline copolymer (LCcoP) with dimethylsiloxane groups in the main chain and nematic LCs have been extensively studied.[14] The smectic (smectic LCcoP/nematic LCs) composite systems exhibited faster electro-optical switching with the bistable memory effect at room temperature in comparison with the smectic (smectic LCP/nematic LC) composite ones, because the smectic LCcoP showed remarkably higher

* To whom correspondence should be addressed. Phone: +81-92-642-3558. Fax: +81-92-651-5606. E-mail: tkajitcf@mbox.nc.kyushu-u.ac.jp.

10.1021/ma980769k CCC: $15.00
Published on Web 10/31/1998

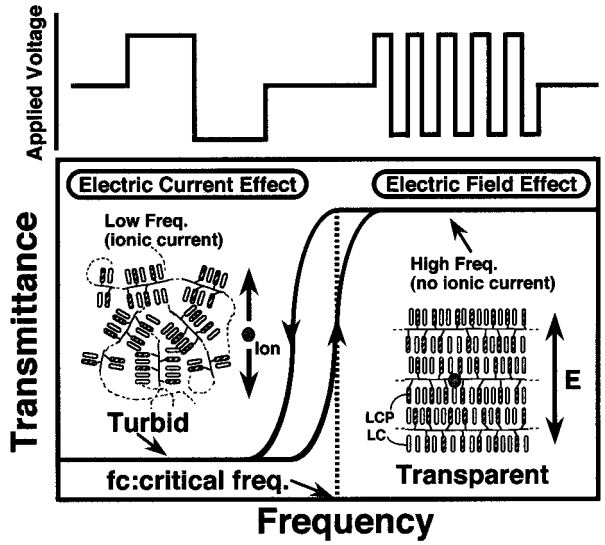

Figure 1. Schematic illustration of the turbid and transparent states for the smectic (LCP/LC) composite system under the application of an ac electric field with different frequencies.

mobility than the smectic LCP at room temperature.[15]

It has been reported that the binary mixtures composed of nematic LCs with a weak polar terminal group and a strong polar end group form an induced smectic phase.[16−19] Then, this concept was applied to the binary composite system of a nematic LCP with a weak polar terminal group in the side chain part and a nematic LC with a strong polar end group in order to reduce the response time for the bistable and reversible light switching.[20] Also, the response speed of the binary composite system in an induced smectic phase could be remarkably improved by an introduction of another LC as the third component, since an addition of the third component of LC made the magnitude of the viscosity in the binary composite system reduced effectively by reducing the LCP fraction. This result apparently indicates that the mechanical stability of an induced smectic state was maintained, even though the LCP was partially replaced by the third component of LC.[21−23] Furthermore, an introduction of LCcoP with a small substituent fraction of mesogenic side chains into the induced smectic binary composite system made the electro-optical switching times with a stable memory effect at room temperature remarkably reduced.[24−27]

In this paper, the influence of the mesogenic side chain fraction in a LCcoP with a strong polar cyano terminal group on the electro-optical effect has been discussed for the smectic (LCcoP/nematic LCs) composite systems in order to improve the reversible and bistable switching speed.

Experimental Section

Materials. Figure 2 shows the chemical structures and physical properties of the smectic LCP, smectic LCcoPs, the pseudo-LCcoP, the dimethylsiloxane copolymer, and nematic LCs used in this study. The LCcoP with the mesogenic side chain fraction 16.5 mol % did not exhibit any mesomorphic characteristics at any temperature without any addition of LCs. Then, such a LCcoP was termed a pseudo-LCcoP in this study. The LCP, the LCcoPs, and the pseudo-LCcoP were poly[(((((4-cyanophenoxy)carbonyl)phenoxy)hexyl)methylsiloxane] homopolymer (PS6EC (n = 24)), poly[(((((4-cyanophenoxy)carbonyl)phenoxy)hexyl)methylsiloxane)-*co*-(dimethylsiloxane)] copolymers (PS(6EC/DM, 52.5/47.5 mol %) (n = 12), PS(6EC/DM, 32.5/67.5 mol %) (n = 27), and PS(6EC/DM, 16.5/83.5 mol %) (n = 29)), respectively. The number of methylene groups used as a flexible alkyl spacer was m = 6. The LCP, LCcoPs, and pseudo-LCcoP with the same mesogenic unit and the siloxane backbone were synthesized through a hydrosilylation reaction between poly[(methylsiloxane)] homopolymer (PHMS) or poly[(methylsiloxane)-*co*-(dimethylsiloxane)] copolymer (PHDS) and the appropriate mesogenic alkene by a conventional method.[28] These chemical structures and the mesogenic side chain fraction in the LCP, the LCcoPs, and the pseudo-LCcoP were confirmed by both NMR and FT-IR. The average degrees of polymerization n, the number- and weight-average molecular weights M_n and M_w, the polydispersity M_w/M_n, and the purities were determined by gel permeation chromatography (GPC) in tetrahydrofuran using polystyrene standards. Also, the dimethylsiloxane copolymer was poly[(methylsiloxane)-*co*-(dimethylsiloxane), 16.5/83.5 mol %] (n = 29) (PHDS (n = 29), Chisso Co. Ltd., PS123.5). The nematic LCs used are the commercial liquid crystalline material E7 (MERCK Co. Ltd., a eutectic nematic mixture). E7 exhibits a positive dielectric anisotropy and is reported to be comprised of cyanobiphenyl, oxycyanobiphenyl, and cyanoterphenyl derivatives.

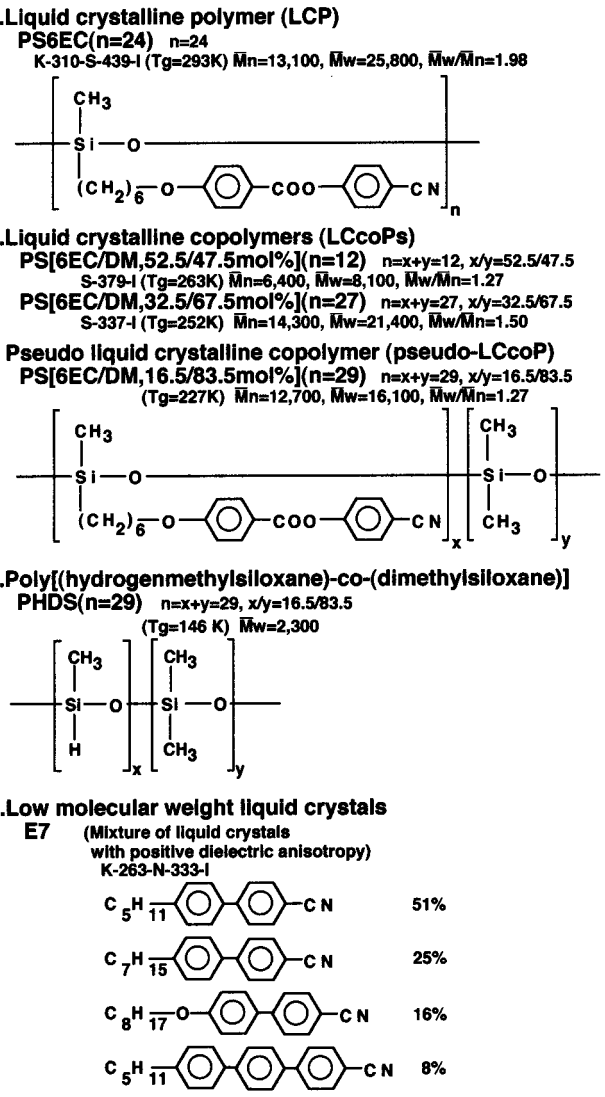

Figure 2. Chemical structures and physical properties of smectic liquid crystalline polymer (1), smectic liquid crystalline copolymers and pseudo liquid crystalline copolymer (2), poly[(methylsiloxane)-*co*-(dimethylsiloxane)] (3), and low-molecular-weight nematic liquid crystals (4).

Characterization of the Binary Composite Systems. The binary composite films were cast from acetone solutions of (LCP/LCs), (LCcoP/LCs), and (pseudo-LCcoP/LCs). The

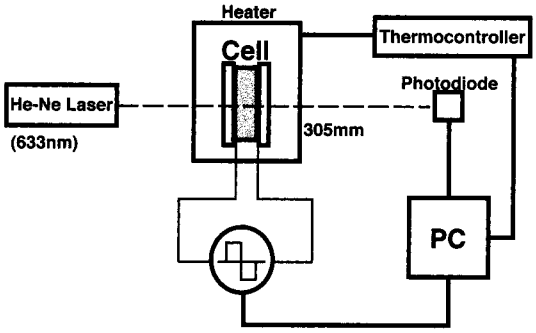

Figure 3. Schematic illustration of the measuring system for electro-optical properties of the composite system.

thermal properties, the phase transition behavior, and the aggregation states of the binary composites were investigated on the basis of differential scanning calorimetry (DSC), polarizing optical microscopy (POM), and X-ray diffraction (WAXD) studies, to obtain the temperature−composition phase diagrams for the binary composite systems. DSC thermograms were obtained under nitrogen purge. To obtain the reproducible DSC data, the third heating curves were used. POM observation was carried out under crossed polarizers by using a hot stage. The heating and cooling rates for DSC studies and POM observations were 5 and 1 K·min^{-1}, respectively. X-ray diffraction patterns were taken on an imaging plate by using Ni-filtered Cu Kα radiation ($\lambda = 0.15405$ nm).

Measurement of Electro-Optical Effect for the Binary Composite Systems. The experimental setup used for electro-optical switching measurements is illustrated in Figure 3. The composite films were sandwiched between two indium−tin oxide (ITO)-coated glass plates of 5 mm × 5 mm which were separated by a PET film spacer 10 μm thick. All samples were measured in an unaligned state. The temperature of the sample was controlled by using a custom-made nichrom heating system attached to a thermocontroller with a resolution of ±0.04 K. A He−Ne laser of 2 mW at 632.8 nm with a beam diameter of 0.63 mm was used as an incident light being transmitted normal to the film surface, and an external ac electric field was applied across the composite film. The transmitted light intensity was measured with a photodiode without any polarizers under the modulation of ac electric fields with two different frequencies, and its effective light detectable area was 6.6 mm^2. The rise response time τ_R was evaluated as the time period required for a 10−90% transmittance change. Similarly, the decay response time τ_D was also evaluated as the time period required for a 90−10% transmittance change. The elapse time dependence of the transmitted light intensity was recorded with a digital storage oscilloscope to evaluate the memory effect of the composite systems. The distance between the cell and the photodiode was 305 mm.

Results and Discussion

Substituent Fraction Dependence of Mesogenic Side Chain on Mesomorphic Characterization of the Smectic Binary Composite Systems. Figure 4 shows the DSC curves and X-ray diffraction patterns of PS6EC ($n = 24$), PS(6EC/DM, 52.5/47.5 mol %) ($n = 12$), PS(6EC/DM, 32.5/67.5 mol %) ($n = 27$), and PS(6EC/DM, 16.5/83.5 mol %) ($n = 29$). The measurements were also made for PHDS ($n = 29$), for which the main chain structure was similar to that of poly(dimethylsiloxane) (PDMS). The glass transition temperatures T_g's of the polysiloxane LCP and the LCcoPs were observed at 293, 263, 252, and 227 K, depending on the mesogenic side chain fraction, as shown by the arrows in Figure 4. In the case of PS(6EC/DM, 16.5/83.5 mol %) ($n = 29$), the second glass transition temperature T_{g2} was measured at 170 K. Also, the apparent glass transition of PHDS ($n = 29$) was at 146

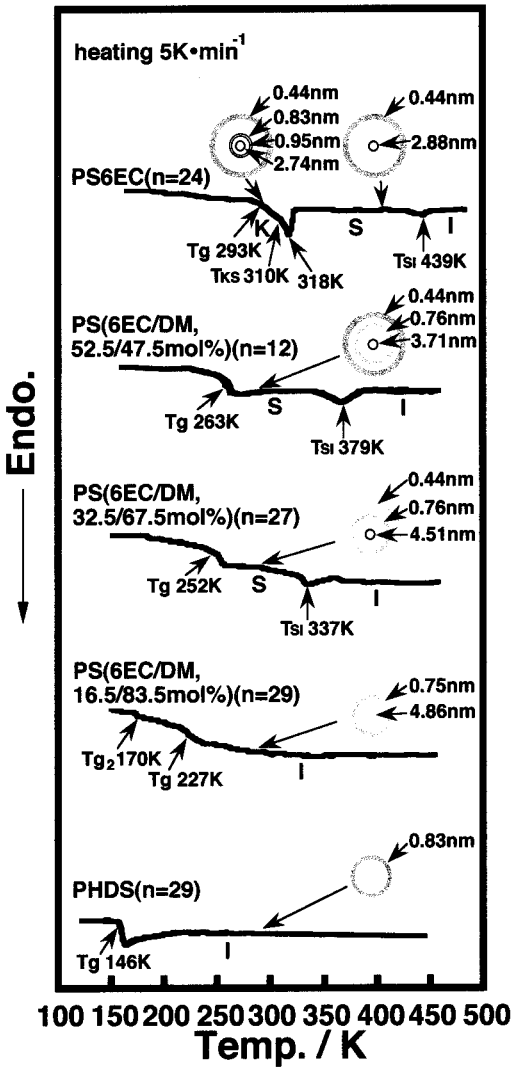

Figure 4. DSC curves and X-ray diffraction patterns of PS6EC ($n = 24$), PS(6EC/DM, 52.5/47.5 mol %) ($n = 12$), PS(6EC/DM, 32.5/67.5 mol %) ($n = 27$), PS(6EC/DM, 16.5/83.5 mol %) ($n = 29$), and PHDS ($n = 29$).

K. The DSC curve of PS6EC ($n = 24$) showed two endothermic peaks corresponding to the crystal−mesophase phase transition temperature T_{KM} at 310 K and the mesophase−isotropic one T_{MI} at 439 K. POM observation of PS6EC ($n = 24$) under crossed nicols showed a fan-shaped texture, which was characteristic of the smectic phase, over the temperature range between T_g and T_{MI}. Also, the X-ray pattern of PS6EC ($n = 24$) at 409 K showed one sharp X-ray scattering corresponding to the spacing 2.88 nm and one diffuse X-ray diffraction corresponding to the spacing 0.45 nm. The sharp small-angle X-ray scattering of 2.88 nm and the diffuse wide-angle X-ray diffraction of 0.44 nm for PS6EC ($n = 24$) might be attributed to the smectic layer structure and the average inter-side-chain distance, respectively. Therefore, T_{KM} and T_{MI} for PS6EC ($n = 24$) may be assigned as the crystal−smectic phase transition temperature T_{KS} and the smectic−isotropic one T_{SI}.

In the case of the PS(6EC/DM, 52.5/47.5 mol %) ($n = 12$) and PS(6EC/DM, 32.5/67.5 mol %) ($n = 27$) films, the DSC curves showed only one endothermic peak corresponding to the mesophase−isotropic phase transition T_{MI} at 379 and 337 K, respectively. POM observation of the PS(6EC/DM, 52.5/47.5 mol %) ($n = 12$) and

PS(6EC/DM, 32.5/67.5 mol %) (n = 27) films under crossed nicols showed a fan-shaped texture characteristic of the smectic phase. The X-ray pattern of the PS(6EC/DM, 52.5/47.5 mol %) (n = 12) film at 293 K exhibited one sharp Debye ring corresponding to the spacing 3.71 nm and two diffuse X-ray diffraction rings corresponding to the spacings 0.76 and 0.44 nm, as shown in Figure 4. Also, the X-ray pattern of the PS(6EC/DM, 32.5/67.5 mol %) (n = 27) film at 293 K showed one sharp Debye ring corresponding to the spacing 4.51 nm and two diffuse X-ray diffraction rings corresponding to the spacings 0.76 and 0.44 nm, respectively. The sharp small-angle X-ray scattering might be attributed to the smectic layer structure. Therefore, the T_{MI}'s for the PS(6EC/DM, 52.5/47.5 mol %) (n = 12) film and the PS(6EC/DM, 32.5/67.5 mol %) (n = 27) one should be assigned as the smectic−isotropic phase transition temperature T_{SI}. On the other hand, in the case of the PS(6EC/DM, 16.5/83.5 mol %) (n = 29) film and the PHDS (n = 29) one, the DSC curves did not show any peaks except the T_g shoulders, as shown in Figure 4. Also, any optical anisotropy was not observed under POM observation in the temperature range studied here. The PS(6EC/DM, 16.5/83.5 mol %) (n = 29) film showed two broad X-ray diffraction halos corresponding to the spacings 4.86 and 0.75 nm. Also, the PHDS (n = 29) film with the dimethylsiloxane main chain showed only one X-ray halo corresponding to the spacing 0.83 nm. Then, it is reasonable to consider that the X-ray halo corresponding to the 0.76 nm spacing for the PS(6EC/DM, 52.5/47.5 mol %) (n = 12), PS(6EC/DM, 32.5/67.5 mol %) (n = 27), and PS(6EC/DM, 16.5/83.5 mol %) (n = 29) films might correspond to the average interchain distance of the siloxane main chain.

It is apparent from Figure 4 that the magnitudes of T_g, T_{MI}, and the mesophase temperature range (MR) of PS(6EC/DM) decreased with a decrease of mesogenic fraction in PS(6EC/DM), in analogy with other side chain type LC polysiloxanes with different substituent fractions of mesogenic side chains (spacer length m = 3, 5, 11) reported by Ringsdorf et al.[29] Therefore, these results apparently indicate that the thermal stability of the smectic phase was reduced with a decrease of the mesogenic side chain fraction and that, then, the main chain backbone becomes more flexible with an increase of the poly(dimethylsiloxane) fraction. Also, PS(6EC/DM) exhibited a broader and lower peak intensity with respect to the small-angle X-ray scattering with a decrease of the 6EC substituent fraction in PS(6EC/DM). This indicates that the smectic ordering of PS(6EC/DM) might be reduced as the mesogenic side chain fraction became lower.

Figure 5 shows the DSC curves and the X-ray diffraction patterns of the (polymer/E7, 40/60 wt %) composite systems. The polymers were PS6EC (n = 24), PS(6EC/DM, 52.5/47.5 mol %) (n = 12), PS(6EC/DM, 32.5/67.5 mol %) (n = 27), PS(6EC/DM, 16.5/83.5 mol %) (n = 29), and PHDS (n = 29). The [PS6EC (n = 24)/E7, 40/60 wt %] composite system showed two endothermic peaks corresponding to the crystal−mesophase phase transition at 276 K (T_{KM}) and the mesophase−isotropic one at 350 K (T_{MI}). POM observation of the binary composite system under crossed nicols showed a schlieren texture characteristic of a nematic phase in the temperature range between T_{KM} and T_{MI}. Also, the X-ray pattern of the composite system at 293 K exhibited two diffuse X-ray diffraction rings corresponding

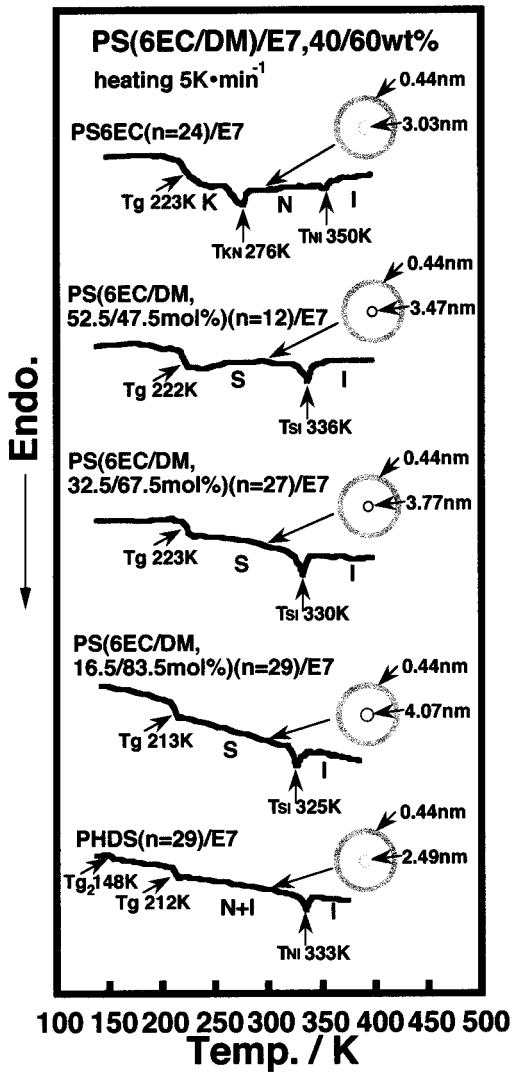

Figure 5. DSC curves and X-ray diffraction patterns of the [PS(6EC/DM)/E7, 40/60 wt %)] composite systems.

to the spacings 3.03 and 0.44 nm. The diffuse small-angle X-ray scattering of the binary composite system might be attributed to the length of mesogenic side chains, that is, the smectic layer. Also, the diffuse wide-angle X-ray diffraction of 0.44 nm might correspond to the average distance among the side chains in the LCP and LC molecules. The X-ray diffraction pattern is characteristic of a nematic phase, since the nematic liquid crystal has a considerable long-range orientational order of the molecules and no long-range translational order. Therefore, T_{KM} and T_{MI} of the [PS6EC (n = 24)/E7, 40/60 wt %] composite system might be assigned as the crystal−nematic phase transition temperature T_{KN} and the nematic−isotropic one T_{NI}, respectively.

In the case of the [PS(6EC/DM, 52.5/47.5 mol %) (n = 12)/E7, 40/60 wt %], [PS(6EC/DM, 32.5/67.5 mol %) (n = 27)/E7, 40/60 wt %], and [PS(6EC/DM, 16.5/83.5 mol %) (n = 29)/E7, 40/60 wt %] composite systems, only one endothermic peak corresponding to T_{MI} was measured at 336, 330, and 325 K, respectively, as shown in Figure 5. These binary composite systems showed the sharp small-angle X-ray scattering corresponding to a smectic layer with the spacings 3.47, 3.77, and 4.07 nm at 293 K, respectively. Also, a fan-shaped texture characteristic of a smectic state was observed under

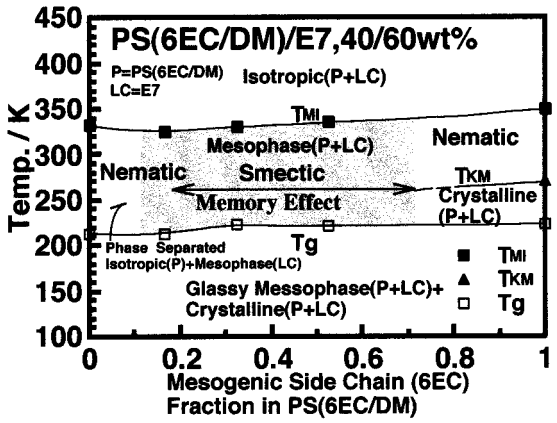

Figure 6. Phase diagram of the [PS(6EC/DM)/E7, 40/60 wt %] composite systems with respect to the mesogenic side chain (6EC) fraction in a PS(6EC/DM) chain.

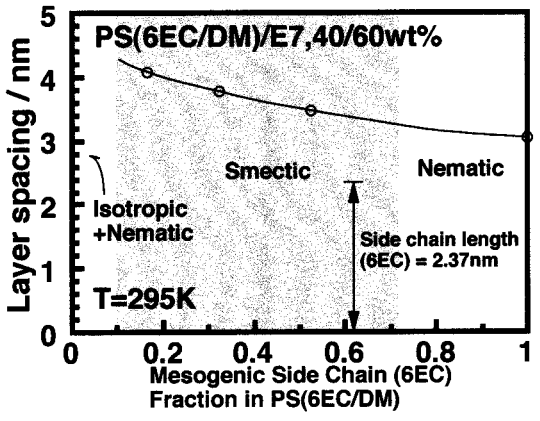

Figure 7. Variation of layer spacing calculated from the small-angle X-ray scattering patterns with the mesogenic side chain (6EC) fraction for the [PS(6EC/DM)/E7, 40/60 wt %] composite systems at 295 K.

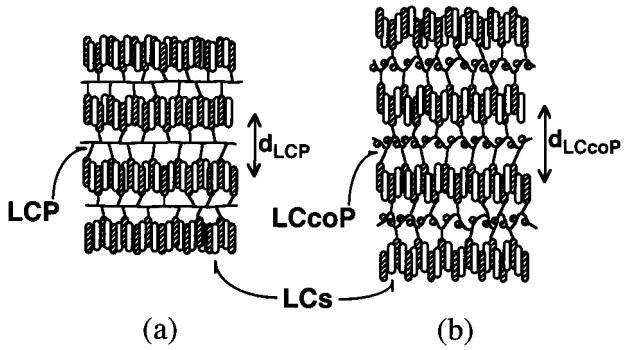

Figure 8. Schematic illustration of the aggregation states for LCP (a) and LCcoP (b) in a smectic phase.

POM in the temperature range between T_g and T_{MI}. These results apparently indicate that these composite systems formed a homogeneous smectic phase. That is, T_{MI} of those composite systems should be assigned as T_{SI}. It is worth noting that though PS(6EC/DM, 16.5/83.5 mol %) (n = 29) did not show any mesophase in the temperature range studied here, as shown in Figure 4, the [PS(6EC/DM, 16.5/83.5 mol %) (n = 29)/E7, 40/60 wt %] composite system showed a homogeneous smectic phase, as shown in Figure 5. Moreover, POM observation recognized that these four composite systems mentioned above exhibited the narrow biphasic mesophase−isotropic coexisting region in a temperature region about 5 K wide below T_{NI} or T_{SI}. On the other hand, the [PHDS (n = 29)/E7, 40/60 wt %] composite system showed only one endothermic peak corresponding to T_{MI} at 333K, which was the same as T_{NI} of E7. POM observation of the binary (PHDS (n = 29)/E7) composite system under crossed nicols showed the phase-separated texture and the schlieren texture characteristic of the nematic E7 phase in the temperature range between T_g and T_{MI}, indicating that PHDS (n = 29) with a dimethylsiloxane main chain was not quite miscible with E7. Also, the X-ray pattern of the composite system at 293 K exhibited two diffuse X-ray diffraction rings corresponding to the spacings 2.49 and 0.44 nm. As mentioned above, these X-ray diffraction patterns are characteristic of the E7 nematic phase.

Figure 6 shows the phase diagram of the [PS(6EC/DM)/E7, 40/60 wt %] binary composite system with respect to the mesogenic side chain (6EC) fraction in a PS(6EC/DM) chain. The phase diagram was drawn on the basis of the results shown in Figure 5. Figure 6 shows that the magnitudes of T_g, T_{MI}, and the mesomorphic temperature range (MR) for the [PS(6EC/DM)/E7] composites were almost independent of the mesogenic side chain fraction in a PS(6EC/DM) chain. It is apparent from DSC, POM, and WAXD studies that the [PS(6EC/DM)/E7, 40/60 wt %] binary composite systems composed of the smectic LCcoPs with the 52.5 and 32.5 mol % mesogenic side chain fractions and the pseudo-LCcoP with the 16.5 mol % one formed a homogeneous smectic phase, while the binary composite system composed of the smectic homo-LCP and PHDS (n = 29) formed a nematic one, as shown in Figure 6. In the case of the [PS(6EC/DM)/E7, 30/70 wt %] binary composite systems, the composite system composed of the smectic LCcoPs with the 52.5 and 32.5 mol % mesogenic side chain fractions showed a homogeneous smectic phase, while the binary composite system composed of the smectic homo-LCP, the pseudo-LCcoP with the 16.5 mol % mesogenic side chain fraction, and PHDS (n = 29) formed a nematic one.

Figure 7 shows the variation of layer spacing calculated from the small-angle X-ray scattering patterns with the mesogenic side chain (6EC) fraction for the [PS(6EC/DM)/E7, 40/60 wt %] composite systems at 295 K. The magnitude of layer spacing corresponding to the smectic layer was longer than the length of the mesogenic side chain (6EC), 2.37 nm under the assumption of the most extending conformation, and shorter than twice the length of 6EC. Also, the layer spacing increased with a decrease of mesogenic side chain fraction. This result may be explained by the degree of interdigitation of the mesogenic side chains (6EC) in the binary composite, as shown in Figure 8. It seems reasonable to consider that since the volume occupied by the main chain of dimethylsiloxane in the PS(6EC/DM) increases, the lateral interaction between the mesogenic side chains becomes weaker with a decrease of the substituent fraction of the 6EC. Therefore, the distance between two siloxane main chains in a smectic layer is more spread, and also, a decrease of the lateral interaction between the mesogenic side chains induces a reduction of the degree of interdigitation of the side chain group from an almost perfect form (a) to a slightly overlapped form (b). These structural variations might make the smectic layer spacing increased with a decrease of the mesogenic side chain fraction, as shown in Figure 7. Also, the spacings of a smectic layer of [PS(6EC/DM)/E7] composite systems were shorter than those of PS(6EC/DM)s without E7, as shown in Figures

4 and 5. The result may be explained as follows. E7 exhibited the diffuse X-ray diffraction ring corresponding to the spacing 2.49 nm. It is well-known that LC cyanobiphenyls, which are strongly polar compounds, show antiparallel local ordering in the nematic and isotropic phases, resulting in a repeat distance along the preferred axis of about 1.4 times the molecular length due to an overlapping head-to-tail arrangement of the neighboring molecules.[30] Though the average length of LC molecules in E7 was almost the same as that of the mesogenic side chain (6EC), 2.37 nm, the magnitudes of the layer spacing of PS(6EC/DM)s were longer than the diffuse X-ray diffraction of E7. For the binary composites, the volume occupied by the main chain of dimethylsiloxane in PS(6EC/DM) decreases, and the lateral interaction between the mesogenic side chains and LC molecules might become stronger with an increase of the mole fraction of E7. Therefore, an increase of the lateral interaction induces a magnification of the degree of interdigitation of the mesogenic side chains and LC molecules, and the spacing of the binary composites decreases to that of an overlapped form of the E7.

In comparison with the [PS(6EC/DM)/E7, 40/60 wt %] binary composite systems, the [PS(6EC/DM, 32.5/67.5 mol %) (n = 27)/E7] composite systems showed the highest peak intensity of the small-angle maximum and, also, exhibited the narrowest half-width of the small-angle X-ray diffraction peak under the assumption of a Lorentzian line shape. In other words, the [PS(6EC/DM, 52.5/47.5 mol %) (n = 12)/E7] and the [PS(6EC/DM, 16.5/83.5 mol %) (n = 29)/E7] composite systems showed the lower peak intensity of the small-angle maximum and, also, exhibited the broader half-width of the small-angle X-ray diffraction peak under the assumption of a Lorentzian line shape with a decrease or an increase of the substituent fraction of 6EC in PS(6EC/DM). This indicates that the [PS(6EC/DM, 32.5/67.5 mol %) (n = 27)/E7] composite system might induce the highest degree of anisotropic LC ordering and that the [PS(6EC/DM)/E7] composite systems might form more disordered smectic layers as the substituted fraction of the mesogenic side chains becomes bigger or smaller than 32.5 mol %.

Figure 9 shows the phase diagrams for the [PS6EC (n = 24)/E7], [PS(6EC/DM, 52.5/47.5 mol %) (n = 12)/E7], [PS(6EC/DM, 32.5/67.5 mol %) (n = 27)/E7], and [PS(6EC/DM, 16.5/83.5 mol %) (n = 29)/E7] composite systems. These phase diagrams were drawn on the basis of DSC and X-ray studies as well as POM observations. The phase diagrams were mainly divided into six regions, that is, (A) isotropic state, (B) biphasic (mesophase + isotropic) state, (C) mesophase (smectic or induced smectic or nematic) state, (D) crystalline (LCP or LCcoP or pseudo-LCcoP + LCs) + mesophase (LCP or LCcoP or pseudo-LCcoP + LCs) state, (E) crystalline (LCP or LCcoP or pseudo-LCcoP + LCs) + glassy mesophase (LCP or LCcoP or pseudo-LCcoP + LCs) state, and (F) phase-separated (isotropic pseudo-LCcoP + mesophase pseudo-LCcoP and LCs) state. The former three phase diagrams of the binary composite systems showed a homogeneous mesophase over the whole mixing concentration of the LCP and the LCcoPs. The C region was a homogeneous mesophase (smectic or nematic) state in which the mixture composed of the smectic LCP, the smectic LCcoPs, or the pseudo-LCcoP and nematic LCs was sufficiently compatible. The magnitude of T_g for the binary composite systems decreased with an increase in the E7 fraction due to the plasticizing effect of E7 to the polymeric chains. Since only one endothermic peak assigned to the mesophase−isotropic transition T_{MI} was obtained by the DSC measurement, no phase-separated texture was recognized in the mesomorphic state under the POM observation, and also, the X-ray diffraction pattern apparently showed Debye rings corresponding to a single component in the mesomorphic state, the binary composite systems might be in a homogeneously mixed mesomorphic phase (a molecularly dispersed state).[11,12] This means that E7 is miscible over a whole concentration range of polysiloxanes in both isotropic and mesomorphic states in the case of the former three composite systems.

The [PS6EC (n = 24)/E7] composite system showed a smectic phase in the range of LCP above 70 wt % (62 mol %), as shown in Figure 9a, while both the [PS(6EC/DM, 52.5/47.5 mol %) (n = 12)/E7] and the [PS(6EC/DM, 32.5/67.5 mol %) (n = 27)/E7] composite systems exhibited a smectic phase over a wide range of both mixing concentration (approximately ∼25 wt % (∼15 mol %) LCcoP fraction) and temperature (250−340 K), as shown in Figure 9b and c. A homogeneous smectic phase played an important role in realizing an excellent bistable memory effect on electro-optical switching due to its considerably high viscosity in comparison with that of a nematic state of E7.[20−25] Moreover, though PS(6EC/DM, 16.5/83.5 mol %) (n = 29) did not exhibit any mesophase characteristics in the temperature range studied here, as mentioned in Figures 4 and 9d, the [PS(6EC/DM, 16.5/83.5 mol %) (n = 29)/E7] composite system showed a homogeneous induced smectic phase over a range of both mixing concentration (85−35 wt % (67−16 mol %) pseudo-LCcoP fraction) and temperature (250−340 K), as shown in Figure 9d. This indicates that though the pseudo-LCcoP is amorphous, its composite system can form an induced smectic phase when E7 is mixed with the amorphous pseudo-LCcoP. Consequently, a novel type of induced smectic binary composite system was realized. Additionally, in the case of the binary composite systems composed of the LCP, the LCcoPs, and the pseudo-LCcoP lower than 40 wt % (32−19 mol %), the mesophase temperature ranges for the binary composite system were independent of the mesogenic side chain fraction in PS(6EC/DM), as shown in Figure 9.

As shown in Figure 9, the (LCcoP/nematic LCs) composite may form a compatible smectic mesophase in wider component and temperature ranges in comparison with those for the (LCP/nematic LCs) one. Namely, an introduction of LCcoP with an appropriate substituent fraction of mesogenic side chain into the binary composite system is extremely effective in order to extend the range of the smectic phase with respect to the component fraction and the applicable temperature near room temperature for the purpose of the electro-optical switching. Therefore, the induced smectic (pseudo-LCcoP/nematic LCs) composite system is expected as the novel type of wide-area LC display with a bistable memory effect and a short response time.

Substituent Fraction Dependence of Mesogenic Side Chain on Electro-optical Properties of the Smectic [PS(6EC/DM)/E7] Composite Systems. Figure 10 shows the relationship between the rise and decay response times τ_R and τ_D and the magnitude of

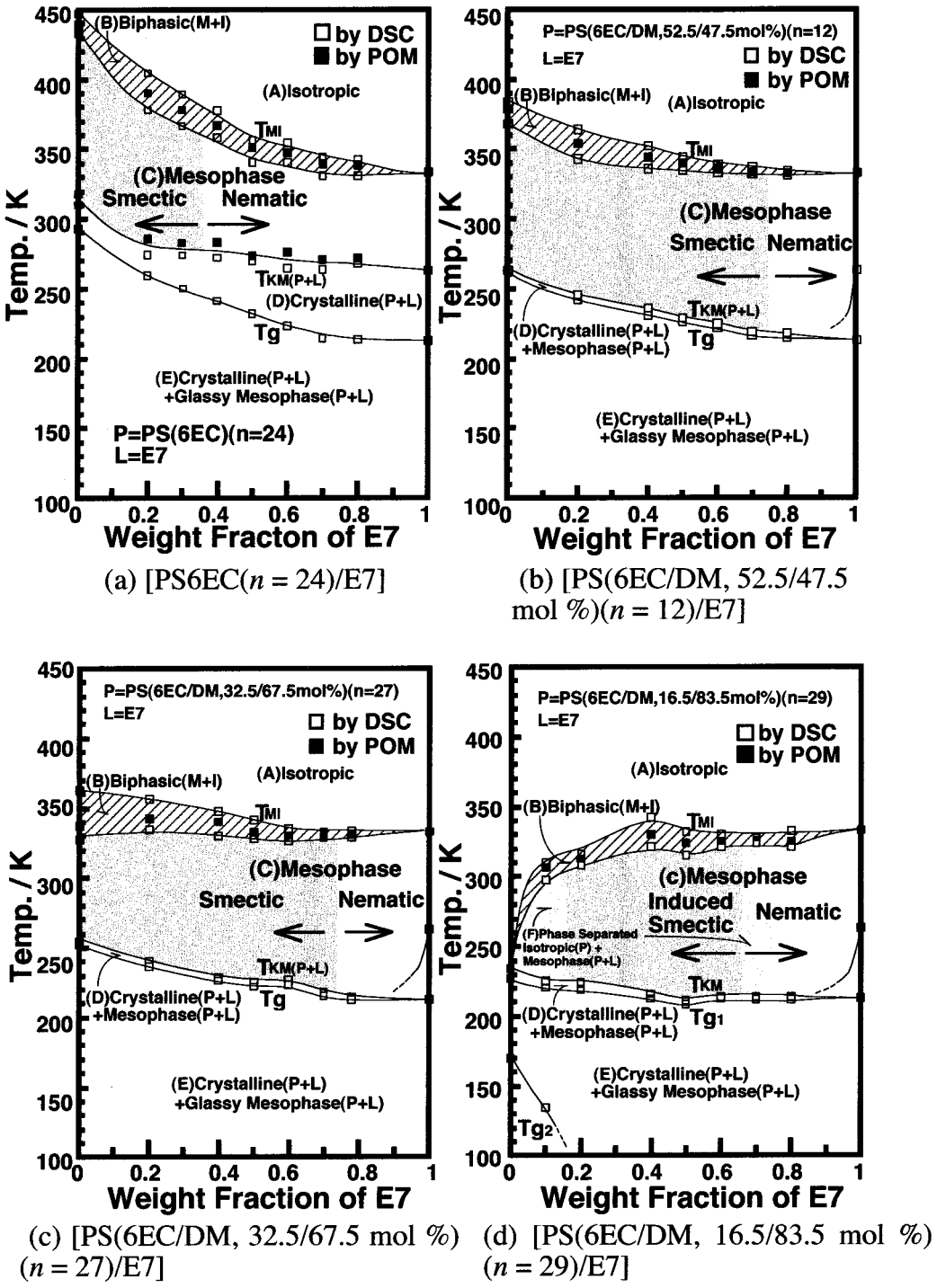

Figure 9. Phase diagrams of the [PS6EC (n = 24)/E7] (a), [PS(6EC/DM, 52.5/47.5 mol %) (n = 12)/E7] (b), [PS(6EC/DM, 32.5/67.5 mol %) (n = 27)/E7] (c), and [PS(6EC/DM, 16.5/83.5 mol %) (n = 29)/E7] (d) composite systems.

the applied electric field E for the [PS(6EC/DM)/E7, 40/60 wt %] (a) and [PS(6EC/DM)/E7, 30/70 wt %] (b) composite systems upon the application of ac electric fields with low (0.1 Hz) and high (1 kHz) driving frequencies at 293 K. The τ_R for the light switching from a transparent state to a light-scattering one was evaluated as the time period required for a 10−90% transmittance change upon the application of an ac electric field with high (1 kHz) driving frequency. Similarly, the τ_D for the light switching from a light-scattering state to a transparent one was also evaluated as the time period required for a 90−10% transmittance change upon the application of an ac electric field with low (0.1 Hz) driving frequency. Parts a and b of Figure 11 also show the relationship between rise and decay response times and mesogenic side chain (6EC) fraction in PS(6EC/DM) for [PS(6EC/DM)/E7, 40/60 wt %] and the [PS(6EC/DM)/E7, 30/70 wt %] composite systems under the electric field strengths 6.25 and 5.00 V_{rms}·μm^{-1} at 293 K, repectively. In the case of the [PS(6EC/DM)/E7, 40/60 wt %] composite systems, since the binary composite systems composed of LCcoPs with the mesogenic side chain fractions 52.5, 32.5, and 16.5 mol % formed a compatible smectic phase, as mentioned in Figure 9, the composite systems exhibited a reversible electro-optical switching with a high contrast (approximately 1−99% transmittance change) as well as a stable memory effect (∼years) at room temperature, in

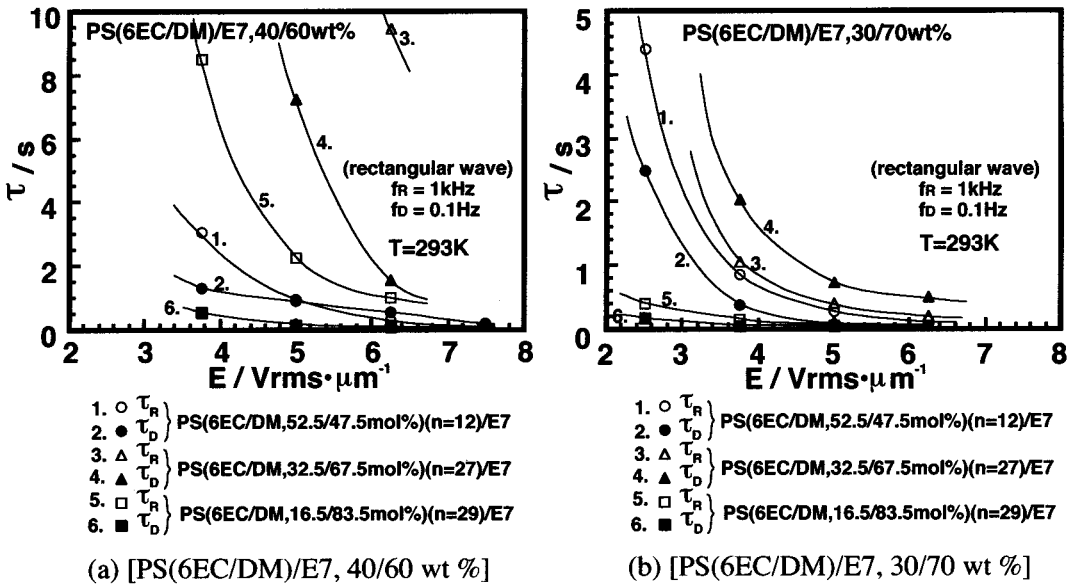

Figure 10. Relationship between the rise and decay response times τ_R and τ_D and the magnitude of the applied electric field E for the [PS(6EC/DM)/E7, 40/60 wt %] (a) and [PS(6EC/DM)/E7, 30/70 wt %] (b) composite systems upon the application of ac electric fields with low (0.1 Hz) and high (1 kHz) driving frequencies at 293 K.

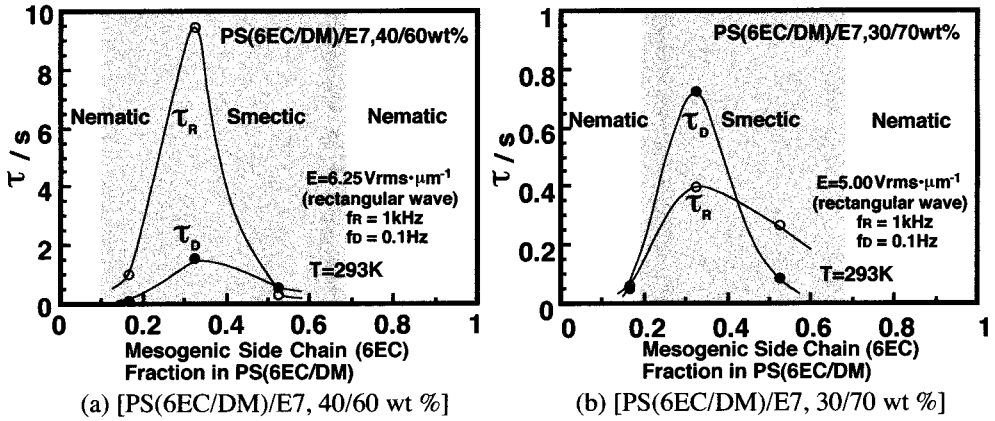

Figure 11. Relationship between the rise and decay response times τ_R and τ_D and the mesogenic side chain (6EC) fraction in PS(6EC/DM) for the [PS(6EC/DM)/E7, 40/60 wt %] (a) and [PS(6EC/DM)/E7, 30/70 wt %] (b) composite systems.

a fashion similar to that for the smectic (LCP/LC) composite systems.[11−15] Also, since the [PS6EC (n = 24)/E7, 40/60 wt %] composite system formed a compatible nematic phase, as shown in Figure 9a, this binary composite did not exhibit a memory effect at room temperature.

The electro-optical switching of the binary composite systems needs the reorientation of polymer segments, as shown in Figure 1. The viscosity and mobility of polymer segments in the binary composites may be closely related to both the length of polymer segments and the mesogenic side chain fraction in the LCcoP. In the previous paper the molecular weight dependence of the electro-optical effect for the binary composite systems was investigated by using LCcoPs, which have the same mesogenic side chain fraction of 52.5 mol %, with 12 and 40 the degrees of polymerzation n, compared with the low-molecular-weight smectic eutectic LCs containing ionic impurity (Pt catalyst) to unify the condition of electric current effect with the composites.[14] The magnitude of τ_R increased with increasing n. The viscosity of the composite system is strongly dependent on the value of n. The increase in τ_R might be due to an increase in the magnitude of viscosity with increasing n. The magnitude of τ_D, however, exhibited a minimum for the LCcoP with n = 12. This result indicates that the LCcoP plays the role of an agitator to enhance the hydrodynamic turbulent flow induced by the ionic current effect. There might be an appropriate length of polymeric main chain to realize an optimum condition for the balance between an electric field effect and an electric current effect. As shown in Figure 2, the molecular weights of the polymers used in this study are not constant. The appearance of the peaks for τ_R and τ_D as shown in Figure 11a might be dependent on the influence of the length of polymer segments on the response behavior.

The appearance of the peaks for τ_R and τ_D as shown in Figure 11a might also be attributed to more regularly organized smectic molecular packing in the [PS(6EC/DM, 32.5/67.5 mol %) (n = 27)/E7, 40/60 wt %] composite system, in comparison with that in other composite systems, as discussed on the basis of X-ray studies.[12,27] Since the magnitude of response times is generally proportional to that of the viscosity in the binary composite system, the viscosity for the reorientational arrangement of the smectic layer fragments might be considerably higher than those of two other composite systems, maybe due to the formation of a more ordered smectic layer. However, the magnitudes of τ_R and τ_D

for the [PS(6EC/DM)/E7, 40/60 wt %] composites ranged over several seconds.

Also, in the case of the [PS(6EC/DM)/E7, 40/60 wt %] binary composite systems composed of PS(6EC/DM)s with the mesogenic side chain fractions 16.5 and 32.5 mol %, the magnitude of τ_D was shorter than that of τ_R, as shown in Figure 11a. On the other hand, in the case of a dynamic scattering mode using low-molecular-weight smectic A LCs doped with a few charged impurities (S_A DSM), the magnitude of τ_D was longer than that of τ_R.[14,31−33] It is reasonable for S_A DSM to consider that a homeotropic−random alignment change corresponding to the variation from laterally large smectic layers to smectic layer fragments was more difficult than the reverse change although the orientational rearrangement of smectic layers in the smectic composite systems was directly influenced by the balance between the electric field effect and the electric current effect. This means that a higher electrical power is necessary for S_A DSM to collapse homeotropic laterally large smectic layers into small smectic fragments in comparison with that for the reverse aggregation change of the smectic layers. However, the magnitude of τ_D of the binary composite system composed of the pseudo-LCcoP with the mesogenic side chain fraction 16.5 mol %, 91 ms, was much shorter than that of τ_R, 1015 ms, and those of τ_D of any other composite systems, as shown in Figure 11a. This apparently indicates that an introduction of the pseudo-LCcoP with a fairly small mesogenic side chain fraction, that is to say, with a fairly large fraction of dimethylsiloxane groups in the main chain, induces the formation of smectic layers with less-ordered molecular packing, resulting in the improvement of the decay response speed.

In the case of the [PS(6EC/DM)/E7, 30/70 wt %] composite systems, the binary composite systems composed of LCcoPs with the mesogenic side chain fractions 32.5 and 52.5 mol % showed a compatible smectic phase, as shown in Figure 9b and c, and exhibited a reversible electro-optical switching with a high contrast (approximately 1−99% transmittance change) as well as a stable memory effect (∼years) at room temperature. In the case of the [PS(6EC/DM, 52.5/47.5 mol %) (n = 12)/E7, 30/70 wt %] composite system, the magnitudes of τ_R and τ_D were 267 and 86 ms, respectively, as shown in Figure 11b. On the other hand, the [PS6EC (n = 24)/E7, 30/70 wt %] composite system showed a compatible nematic phase at room temperature and exhibited no memory effect at any temperature. In the case of the [PS(6EC/DM, 16.5/83.5 mol %) (n = 29)/E7, 30/70 wt %] composite system, the binary composite system did not exhibit any memory effect at any temperature but showed a reversible electro-optical switching with a high contrast due to the formation of a phase-separated nematic phase. The magnitudes of τ_R and τ_D were 59 and 51 ms, respectively, as shown in Figure 11b.

As discussed above, it is necessary to reduce the weight fraction of LCcoP in the (LCcoP/LCs) binary composite system in order to improve the electro-optical switching speed. Therefore, an appropriate introduction of flexible dimethylsiloxane segments into a rigid LCcoP main chain might be permissible to reduce the magnitudes of τ_R and τ_D, because the smectic phase in the binary composite system can be formed despite the use of the small fraction of LCcoP. Then, it can be concluded that the LCcoP with the optimum substituted fraction of mesogenic side chains is required to realize fairly fast electro-optical switching (∼50 ms) as well as the stable memory (∼years) at room temperature.

Conclusions

The influence of the mesogenic side chain fraction in the LCcoP on the mesomorphic characteristic and electro-optical properties of the (LCcoP/LCs) binary composite systems has been investigated. In the case of the composite system composed of LCP or LCcoPs lower than 40 wt %, the glass transition temperature T_g and the mesophase temperature range MR for the composite system were independent of the mesogenic side chain fraction in the LCP or LCcoPs, that is, 220−340 K. The binary (LCcoP/nematic LCs, 30/70 wt %) composite systems composed of LCcoPs with the mesogenic side chain fractions 32.5 and 52.5 mol % showed a compatible smectic phase at room temperature. The introduction of the LCcoPs with an appropriate mesogenic side chain fraction into the binary composite system was strikingly effective to reduce the electro-optical switching times with a stable memory effect at room temperature due to an apparent reduction of the LCcoP fraction, maintaining a smectic mesophase range near room temperature widely. The pseudo-LCcoP with the mesogenic side chain fraction 16.5 mol % in the main chain did not exhibit any mesophase characteristics. However, the binary composite showed an induced smectic phase over a wide range of both mixing concentration (35−75 mol % LCcoP) and temperature (220−320 K). The novel type of phase diagram for an induced smectic binary composite system composed of the pseudo-LCcoP with a strong polar terminal cyano group in the side chains and nematic LCs with the same terminal group, that is, an induced smectic (pseudo-LCcoP/nematic LCs) composite system, was developed. This system showed a higher bistable light-switching speed from the transparency state to the light-scattering one. This indicates that the LCcoP with the optimum substituent fraction of mesogenic side chain is required to realize a higher speed of electro-optical switching (∼50 ms) as well as a stable memory effect (∼years).

References and Notes

(1) McArdle, C. B., Ed. In *Side Chain Liquid Crystal Polymers*; Blackie: Glasgow and London, Chapman and Hall, Inc.: New York, 1989.
(2) Shibaev, V. P.; Kostromin, S. G.; Plate, N. A.; Ivanov, S. A.; Vetrov, V. Yu.; Yakoviev, I. A. *Polym. Commun.* **1983**, *24*, 364.
(3) Simon, R.; Cole, H. J. *Mol. Cryst. Liq. Cryst.* **1984**, *102*, 43. Cole, H. J.; Simon, R. *Polymer* **1985**, *26*, 1801.
(4) Ueno, T.; Nakamura, T.; Tani, C. *Proc. Jpn. Disp.* **1986**, 190.
(5) Coles, H.; Simon, R. In *Recent Advances in Liquid Crystalline Polymers*; Chapoy, L., Ed.; Elsevier Applied Science: London, 1985.
(6) Coles, H.; Simon, R. *Mol. Cryst. Liq. Cryst.* **1985**, *1*, 75.
(7) Coles, H.; Simon, R. *Mol. Cryst. Liq. Cryst.* **1986**, *3*, 37.
(8) McArdle, C.; Clark, M.; Haws, C.; Wiltshire, M.; Parker, A.; Nestor, G.; Gray, G.; Lacey, D.; Toyne, K. *Liq. Cryst.* **1987**, *2*, 573.
(9) Hopwood, A. I.; Coles, H. J. *Polymer* **1985**, *26*, 1312.
(10) Sefton, M. S.; Coles, H. J. *Polymer* **1985**, *26*, 1319.
(11) Kajiyama, T.; Kikuchi, H.; Miyamoto, A.; Moritomi, S.; Hwang, J. C. *Chem. Lett.* **1989**, *1989*, 817−820.
(12) Kikuchi, H.; Moritomi, S.; Hwang, J. C.; Kajiyama, T. *Polym. Adv. Technol.* **1990**, *1*, 297−300.
(13) Kajiyama, T.; Kikuchi, H.; Hwang, J. C.; Miyamoto, A.; Moritomi, S.; Morimura, Y. *Prog. Pac. Polym. Sci.* **1991**, 343−354.
(14) Kajiyama, T.; Yamane, H.; Kikuchi, H.; Hwang, J. C. In *Liquid-Crystalline Polymer Systems Technological Advances*; Isayev, A. I., Kyu, T., Cheng, S. Z. D., Eds.; ACS Symposium

Series No. 632; American Chemical Society: Washington, DC, 1996; Chapter 12, p 190.
(15) Yamane, H.; Kikuchi, H.; Kajiyama, T. *Polym. Prepr., Jpn.* **1992**, *41*, 3719−3721.
(16) Griffin, A. C.; Johnson, J. F. *J. Am. Chem. Soc.* **1977**, *99*, 4859.
(17) Engelen, B.; Heppke, G.; Hopf, R.; Schnider, F. *Ann. Phys.* **1978**, *3*, 403.
(18) Domon, M.; Billard, J. *J. Phys. (Paris)* **1979**, *40*, C3−413.
(19) Schneider, F.; Sharna, N. K. *Z. Naturforsch.* **1981**, *36*, 62.
(20) Kajiyama, T.; Kikuchi, H.; Miyamoto, A.; Moritomi, S.; Hwang, J. C. *Mater. Res. Soc. Symp. Proc.* **1990**, *171*, 305.
(21) Hwang, J. C.; Kikuchi, H.; Kajiyama, T. *Polymer* **1992**, *33*, 1822−1825.
(22) Hwang, J. C.; Kikuchi, H.; Kajiyama, T. *Polym. J.* **1995**, *27*, 292−299.
(23) Kajiyama, T.; Kikuchi, H.; Hwang, J. C.; Yamane, H. *Polym. Mater. Sci. Eng.* **1995**, *72*, 490−491.
(24) Yamane, H.; Kikuchi, H.; Kajiyama, T. *Trans. Mater. Res. Soc. Jpn.* **1996**, *20*, 307−310.
(25) Kajiyama, T.; Yamane, H.; Kikuchi, H. *Trans. Mater. Res. Soc. Jpn.* **1996**, *32*, 48−51.
(26) Kajiyama, T.; Yamane, H.; Kikuchi, H. *Proc. SPIE* **1997**, *3015*, 125−133.
(27) Yamane, H.; Kikuchi, H.; Kajiyama, T. *Macromolecules* **1997**, *30* (11), 3234−3241.
(28) Finkelmann, H.; Rehage, G. *Makromol. Chem. Rapid. Commun.* **1980**, *1*, 31−34.
(29) Ringsdorf, H.; Schneller, A. *Makromol. Chem. Rapid Commun.* **1982**, *3*, 557.
(30) Leadbetter, A. J.; Richardson, R. M.; Colling, C. N. *J. Phys.* **1975**, *36*, C1−37.
(31) Tani, C. *Appl. Phys. Lett.* **1971**, *19* (7), 241.
(32) Coates, D. *J. Phys. D: Appl. Phys.* **1978**, *11*, 2025.
(33) Crossland, W. A. *SID'85 Digest*. **1985**, 124.

MA980769K